for four values of κ/β. Three of these values correspond to $s < 1.3$, and the corresponding values of $P_a(L)$ lie close to both the $\langle | T |^2 \rangle$ and $W_a(0)$ curves. The fourth value of $2\pi\kappa/\beta$ is 3 (for which ϵ is not very small), which corresponds to $s = 11.4$, and lies outside the range of s in Fig. 1.

Since the above experimental values give only one comparison point in the region in which $W_a(0)$ and $\langle | T |^2 \rangle$ are not close, Marcuse [10], at the request of the author, carried out some more computer simulated experiments in the case $N = 500$. The additional points are indicated by circles in Fig. 1. The values for $s = 8.37$ and $s = 9.12$ were obtained by averaging over 40 waveguides, rather than 10, because of the large scatter for these values of s. The experimental values tend to confirm the validity of the asymptotic value $\langle | T |^2 \rangle$ of the average output power, given by (51), subject to (12) and (50). We emphasize that the asymptotic result holds for quite general weak zero-mean wide sense stationary coupling.

Also depicted in Fig. 1 is the quantity $\langle | T |^{-2} \rangle^{-1}$. From (21) and (22), note that $| T |^{-2}$ is the value of the input power $| a(L) |^2$, when the output power $| a(0) |^2$ is unity. From (50), (52), and (55), it follows that

$$\langle | T |^{-2} \rangle^{-1} = \frac{2}{(1 + e^{2s})} . \tag{58}$$

Although $\langle | T |^{-2} \rangle^{-1}$ has the same initial slope as $\langle | T |^2 \rangle$, it is seen that it decreases very much more rapidly with increasing s.

Acknowledgment

The author wishes to thank D. Marcuse for carrying out some additional computer simulated experiments.

References

[1] D. Marcuse, "Coupled power equations for backward waves," *IEEE Trans. Microwave Theory Tech.*, vol. MTT-20, pp. 541–546, Aug. 1972.
[2] G. C. Papanicolaou, "A kinetic theory for power transfer in stochastic systems," *J. Math. Phys.*, vol. 13, pp. 1912–1918, Dec. 1972.
[3] G. C. Papanicolaou and J. B. Keller, "Stochastic differential equations with applications to random harmonic oscillators and wave propagation in random media," *SIAM J. Appl. Math.*, vol. 21, pp. 287–305, Sept. 1971.
[4] R. Z. Khas'minskii, "A limit theorem for the solutions of differential equations with random right-hand sides," *Theory Prob. Appl.*, vol. 11, pp. 390–406, 1966.
[5] W. Feller, *An Introduction to Probability Theory and Its Applications*, vol. II. New York: Wiley, 1966, p. 586.
[6] G. C. Papanicolaou, "Wave propagation in a one-dimensional random medium," *SIAM J. Appl. Math.*, vol. 21, pp. 13–18, July 1971.
[7] I. I. Gikhman and A. V. Skorokhod, *Introduction to the Theory of Random Processes*. Philadelphia, Pa.: Saunders, 1969, p. 377.
[8] J. A. Morrison, G. C. Papanicolaou, and J. B. Keller, "Mean power transmission through a slab of random medium," *Commun. Pure Appl. Math.*, vol. 24, pp. 473–489, July 1971.
[9] J. A. Morrison, "Application of a limit theorem to solutions of a stochastic differential equation," *J. Math. Anal. Appl.*, vol. 39, pp. 13–36, July 1972.
[10] D. Marcuse, private communication.

Short Papers

Ridged Circular Waveguide

YIH SHIAU AND RICHARD F. H. YANG, FELLOW, IEEE

***Abstract*—Characteristics of wave propagation inside a ridged circular waveguide are studied. The waveguide is a hollow, conducting circular cylinder with a pair of semicircular conducting ridges diametrically attached to its inside wall. Results of a perturbation analysis suggest that in this device a lower attenuation and a wider bandwidth than those of a conventional circular waveguide can be achieved. Certain numerical results are graphically presented.**

Introduction

It has been found experimentally that, in a seam-weld circular waveguide, the polarization of the dominant TE_{11} wave or the orientation of the line joining the two E_ρ maxima wanders, and the wave has a great tendency to orient its E_ρ maximum along the seam ridges [1]. Further experimentation indicated that this tendency was pronounced for a thick seam or with a seam intended inward to form a semicircular ridge. In this study, an analysis is made of the characteristic of wave propagation in a hollow, conducting circular cylinder with a pair of semicircular conducting longitudinal ridges diametrically attached to its inside wall.

To solve this problem as an exact boundary-value problem, the process is long and quite complicated. Instead, a formulation based on perturbation theory is used. The result is expected to be quite good for small ridges with smooth cross sections.

Cutoff Frequency

Let us consider a ridged circular waveguide with its longitudinal axis in the z direction of a cylindrical coordinate system. The symmetric ridge-pair assumed to have a semicircular cross section is shown in Fig. 1, where θ is defined as the angle between the longitudinal plane bisecting the ridge-pair (ridge-pair plane) and the longitudinal plane containing the two E_ρ maxima (polarization).

The ridged circular waveguide may be considered as a smooth waveguide with its boundary wall perturbed by a symmetric ridge-pair along the longitudinal direction. It is well known that the time average of stored magnetic and electric energies are equal in a waveguide at cutoff frequency. A small deformation in the waveguide wall will cause an unbalance in these energies. Therefore, the cutoff frequency will have to shift by an amouut necessary to reequalize

Manuscript received December 31, 1972; revised August 10, 1973. This work was supported by the Aileen S. Andrew Foundation, Orland Park, Ill. 60462.
The authors are with the Department of Electrical Engineering, Illinois Institute of Technology, Chicago, Ill. 60616.

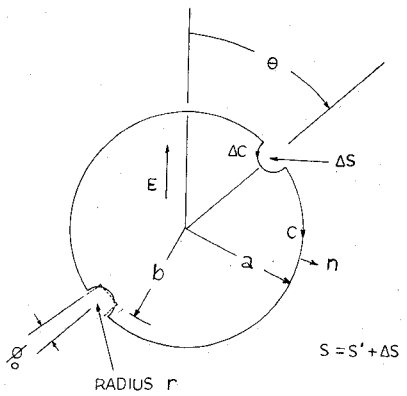

Fig. 1. The cross section of a ridged circular waveguide.

these energies. According to an approximate relationship, the frequency shift is given by [2]

$$\frac{f_c - f_0}{f_0} = \iint_{\Delta S} [\mu|H_0|^2 - \epsilon|E_0|^2]\,ds \Big/ \iint_{S} [\mu|H_0|^2 + \epsilon|E_0|^2]\,ds. \quad (1)$$

In this expression, ΔS and S are, respectively, the cross sections of the ridge-pair and the smooth waveguide; μ and ϵ are the permeability and permittivity; E_0 and H_0 are the electric and magnetic fields in the waveguide with the ridge-pair being removed; f_c and f_0 are, respectively, the cutoff frequencies with and without the ridge-pair. In evaluating (1), ΔS can be further approximated by an equal area trapezoidal sector as shown by the dotted lines in Fig. 1. The criterion used here is to choose a value of normalized ridge radius r/a such that the following two conditions are satisfied:

$$r^2 = \phi_0(a^2 - b^2)\,(2/\pi) \qquad a - b = a\phi_0 \quad (2)$$

where a is the radius of the ridged waveguide and ϕ_0 is the half-angle subtended by the sector in radians. As an example, the energy in the volume occupied by a ridge of radius $r = 0.214a$ is approximated by the energy in a sector with $\phi_0 = 0.2$ rad and $b/a = 0.8$. Substitution of the field solutions of E_0 and H_0 into (1) yields an approximate normalized cutoff frequency of TM_{01} mode

$$\frac{f_c}{f_0} = 1 + 0.985[\phi_0(b/a)J_0(X_1)J_1(X_1)] \quad (2)$$

where $X_1 = 2.405(b/a)$ and $J_n(X)$ is the nth order Bessel function of the first kind. Similarly, the cutoff frequency of the dominant TE_{11} mode for $\theta = 90°$ is obtained as

$$\frac{f_c}{f_0} = 1 + 0.7925(\phi_0[X_1J_0(X_2)J_1(X_2) - J_1^2(X_2)] + \tfrac{1}{2}\sin(2\phi_0)[J_0^2(X_2) + J_0(X_2)J_1(X_2) - 0.44]) \quad (4)$$

where $X_2 = 1.84(b/a)$. For $\theta = 0°$ and $\theta = 45°$, the normalized cutoff frequencies of TE_{11} mode are, respectively,

$$\frac{f_c}{f_0} = 1 + 0.7925(\phi_0[X_2J_0(X_2)J_1(X_2) - J_1^2(X_2)] - \tfrac{1}{2}\sin(2\phi_0)[J_0^2(X_2) + J_0(X_2)J_1(X_2) - 0.44]), \qquad (\theta = 0°) \quad (5)$$

$$\frac{f_c}{f_0} = 1 + 0.7925(\phi_0[X_2J_0(X_2)J_1(X_2) - J_1^2(X_2)]), \qquad (\theta = 45°). \quad (6)$$

In these expressions, the cutoff frequencies are in terms of the sector parameters ϕ_0 and (b/a). By using the relations (2), the cutoff frequencies versus ridge radius (r/a) are calculated.

For $\theta = 0°$, the cutoff frequency of a TE_{11} wave decreases with increasing ridge radius r. For $\theta = 90°$ and $\theta = 45°$, the converse is true. The cutoff frequency of TM_{01} mode also increases as r increases, but is not a function of θ, because of its circular mode symmetry. These results are plotted in Fig. 2. In a ridged circular waveguide,

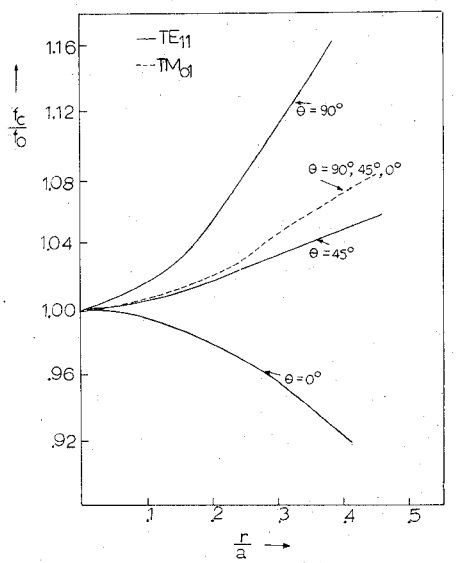

Fig. 2. Normalized cutoff frequency of ridged circular waveguide.

the cutoff frequency is decreased for the dominant TE_{11} mode with $\theta = 0$, and is increased for the next lowest cutoff TM_{01} mode. Therefore, the useful frequency bandwidth of a ridged circular waveguide is wider than that of a smooth waveguide.

Waveguide Attenuation

The attenuation constant of a waveguide is given by the following expression [3]:

$$\alpha = R_S \oint_c |H_t|^2\,dl \Big/ 2\iint_S [\boldsymbol{E} \times \boldsymbol{H}^*]\cdot d\boldsymbol{s}. \quad (7)$$

In this expression, R_S is the surface resistance of the waveguide wall, H_t is the magnetic field tangential to the waveguide wall, and c is the periphery of the waveguide cross section. General solution of the above expression in terms of Bessel functions is somewhat complicated. However, for certain specific cases of interest, the result can be evaluated individually. Assuming relations (2), the following expressions are obtained for $r = 0.21a$:

$$\alpha_{TM} = \left[\frac{7.31 \times 10^{-10} f^{1/2}}{a}\right]\left[\frac{1}{[1 - (f_c/f)^2]^{1/2}}\right] \quad (8)$$

$$\alpha_{TE} = \left[\frac{R_S}{aZ_0}\right]\left[\frac{0.427 + 1.237(f_c/f)^2}{[1 - (f_c/f)^2]^{1/2}}\right] \quad (9)$$

for $\theta = 90°$ and

$$\alpha_{TE} = \left[\frac{R_S}{aZ_0}\right]\left[\frac{0.452 + 1.046(f_c/f)^2}{[1 - (f_c/f)^2]^{1/2}}\right] \quad (10)$$

for $\theta = 0°$, where $Z_0 = (\mu_0/\epsilon_0)^{1/2}$.

The attenuation factors as a function of frequency are shown in Fig. 3 for TE_{11} wave with $\theta = 0$ and TM_{10} wave. The losses for these two modes of a smooth waveguide are also plotted in Fig. 3 for comparison. Radii of ridged and smooth circular waveguides denoted by a and a_s are, respectively, chosen to be $a = 2.54$ cm and $a_s = 2.49$ cm, so that they have a same cutoff frequency for the TM_{01} mode. As shown in Fig. 3, the ridged waveguide has a lower loss for the dominant TE_{11} mode than that of the smooth circular waveguide in the normal operating frequency band.

In a ridged circular waveguide, wave attenuation also depends on the orientation of the ridge-pair plane with respect to wave polarization. The attenuation is minimum when $\theta = 0°$ and becomes maximum when $\theta = 90°$. This fact may explain why wave polarization is most stable in the $\theta = 0°$ orientation. The attenuation factors of TE_{11} waves versus frequency for these two orientations are plotted in Fig. 4 for comparison.

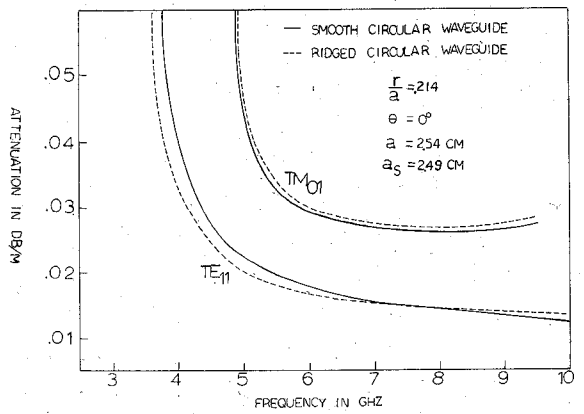

Fig. 3. Attenuation of TE_{11} and TM_{01} waves versus frequency.

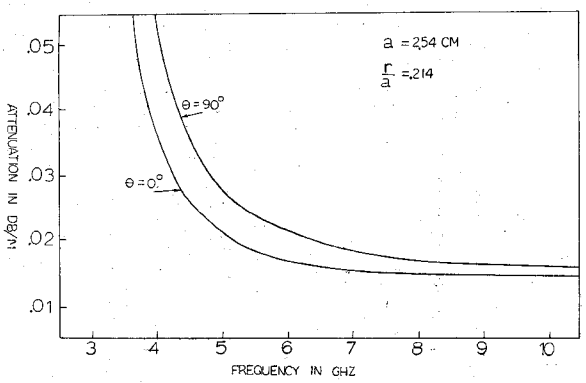

Fig. 4. Comparison of attenuation of TE_{11} wave for $\theta = 0°$ and $\theta = 90°$.

Conclusion

The cutoff frequencies and attenuation of waves in a ridged circular waveguide are calculated. The results suggest that a ridged circular waveguide has a lower loss and larger bandwidth than those of a smooth circular waveguide for the dominant TE_{11} wave polarized in ridge-pair plane in the normal operating band. Attentuation of TE_{11} wave in a ridged circular waveguide is minimum when the wave is polarized in the ridge-pair plane ($\theta = 0°$) and is maximum when the wave is polarized normal to the ridge-pair plane ($\theta = 90°$).

Conclusions reached here are drawn from the calculations of a formulation based on perturbation theory. The results do not hold for large r/a, however. Since the exact field distribution within the waveguide is unknown, error can only be estimated. For design purposes, however, the error can be estimated for a fixed r/a on the basis of a comparison between (1) and the more exact solutions [4], [5] for a rectangular waveguide with a same wall-deformation. For example, the cutoff frequency-shift based on (1) is calculated in a rectangular waveguide with a rectangular longitudinal ridge attached in the H plane with dimensions corresponding to $r/a = 0.275$ in Fig. 2. The result is then compared to that of Cohn's work [4] and an error is obtained. If this same error is assumed for the case of ridged circular guide, then the cutoff frequency-shift is estimated to be within 0.65 percent for TE_{11} mode and 0.77 percent for TM_{01} mode. For a circular ridge which is the case in this study, the result is expected to be somewhat better, because of the smoothness of the wall-boundary, although a complete error analysis for the wide range of r/a in Figs. 2–4 has not been carried out.

References

[1] T. Charlton, Andrew Corporation, Orland Park, Ill., private communication, Jan. 1970.
[2] R. F. Harrington, *Time Harmonic Electromagnetic Fields*. New York: McGraw-Hill, 1961, p. 327.
[3] S. Ramo and J. R. Whinnery, *Fields and Waves in Modern Radio*. New York: Wiley, 1965, p. 405.
[4] S. B. Cohn, "Properties of ridged wave guide," *Proc. IRE*, vol. 35, pp. 783–788, Aug. 1947.
[5] E. V. Juhl, W. J. Bleackley, and M. M. Steen, "The design of waveguides with symmetrically placed double ridges," *IEEE Trans. Microwave Theory Tech.*, vol. MTT-17, pp. 397–399, July 1969.

Magnetostatic Surface Waves in Ferrite Slab Adjacent to Semiconductor

MASAMITSU MASUDA, MEMBER, IEEE, NION S. CHANG, MEMBER, IEEE, AND YUKITO MATSUO

***Abstract*—Magnetostatic surface waves propagating along the ferrite slab adjacent to a semiconductor are discussed in this paper. Our numerical results indicate that the conductivity of the semiconductor plays an important role in the determination of the dispersion relation in the case of nondrifting carriers. The backward wave appears for a finite value of the conductivity.**

I. Introduction

Magnetostatic modes propagating along a ferromagnetic slab in free space were first examined by Damon and Eshbach [1] (DE waves). Applying a dc magnetic field transverse to the direction of the wave propagation, the surface wave which corresponds to the $\theta = 90°$ spin wave is excited. This wave is unique to the slab configuration. Seshadri [2] considered the case where a metal conductor was placed on one face of the slab. Such a grounded ferrite slab has two different surface waves which propagate in opposite direction to each other. Both surface waves are forward modes. Subsequently, Bongianni [3] discussed magnetostatic waves in the dielectric-layered structure where the dielectric material was between a YIG film and a perfect conductor. A backward wave appears at some value of the thickness of the dielectric layer. On the other hand, the general theory of the surface wave on a metallized ferrite film, including dipolar, exchange, and conductivity effects, has been treated by Wolfram and DeWames [4].

Our interest is not only in the behavior of the magnetostatic waves but also in the wave interaction between the ferrite and the semiconductor. It has been suggested that the solid-state traveling wave amplifier (STWA) can be constructed with a layered structure containing both materials [5]–[7]. A detailed understanding of the coupling of the spin wave in ferrite and the carrier wave in semiconductor is important for the design of STWA. Preliminary to a discussion of the amplification process, we deal in the present paper with the magnetostatic surface waves propagating along a ferrite slab adjacent to a semiconductor. The finite conductivity of the semiconductor gives us remarkable changes to the properties of the surface waves. The dispersion relationship can be obtained by solving the boundary value problem for three regions of ferrite, semiconductor, and free space.

II. Analysis

The geometry treated in this paper is a layered structure constituted by a ferrite slab and a semiconductor layer in free space, as shown in Fig. 1. The external dc magnetic field is applied parallel to the y direction. The propagating directions of magnetostatic surface waves and the carrier flow in the semiconductor are chosen to be in the z direction. Our two-dimensional analysis is based on the assumptions that the wave varies as $\exp j(\omega t - \beta z)$ and that all properties are independent of y ($\partial/\partial y = 0$).

The field components in the semiconductor region, which is a collision-dominated system for electrons, satisfy the following equations:

$$\nabla \times \boldsymbol{H} = \boldsymbol{J} + j\omega\epsilon_s \boldsymbol{E} \tag{1}$$

$$\nabla \times \boldsymbol{E} = -j\omega\mu_0 \boldsymbol{H} \tag{2}$$

$$\nabla \times \boldsymbol{E} = \rho/\epsilon_s \tag{3}$$

$$\boldsymbol{J} = \rho_0 \boldsymbol{V} + \rho \boldsymbol{V}_0 \tag{4}$$

$$\boldsymbol{V} = \bar{\mu}_s(\boldsymbol{E} + \boldsymbol{V} \times \boldsymbol{B}_0 + \boldsymbol{V}_0 \times \boldsymbol{B}) \tag{5}$$

$$\bar{\mu}_s = \begin{vmatrix} \mu_t & 0 & 0 \\ 0 & \mu_t & 0 \\ 0 & 0 & \mu_z \end{vmatrix}, \qquad \mu_t = v/E, \quad \mu_z = \partial v/\partial E \tag{6}$$

Manuscript received March 5, 1973; revised September 17, 1973.
The authors are with the Institute of Scientific and Industrial Reseach, Osaka University, Osaka, Japan.